Experimental Investigation of CO_2 Buoyant Flow Saturation: The Impact of Realistic Bedforms and Heterogeneous Wettability

J. E. Ubillus[1,2], **H. Ni**[2], **D. DiCarlo**[1]

[1]Hildebrand Department of Petroleum and Geosystems Engineering, The University of Texas at Austin
[2]Bureau of Economic Geologic, The University of Texas at Austin

Key Points:

- Bedform architecture modifications and wettability changes can significantly impact nonwetting saturation and capillary heterogeneity trapping.

Corresponding author: Hailun Ni, `hailun.ni@beg.utexas.edu`

Abstract

We produce realistic sedimentary formations consisting of ripple deposits with varying grain size contrast and wettability in a meter-scale slab chamber. Then, we conduct multiphase flow experiments through these structures and measure the infiltration patterns, capillary heterogeneity trapping, and overall trapping performance. When we alter the ripple bedform architecture, variations in trapped saturation and capillary heterogeneity trapping (10% to 20%) increment are exhibited. Similar growth in trapping performance is also observed when grain size contrast increases. Finally, wettability changes (water- to oil-wet) can increase nonwetting saturation and capillary heterogeneity trapping up to 5% and 10-20%, respectively. These results emphasize the importance of correctly characterizing the impact of small-scale heterogeneities and wettability changes.

Plain Language Summary

We make sediment layers in a 60-cm tank. These layers look like the ones you would find in real Earth formations. Then, we conduct the flow experiment through these layers to see how they affect the fluid movement. We look at how the fluid spread out and get trapped in the layers. Depending on how we arrange the ripples in the layers, we notice that more liquid gets trapped in certain places. Also, when we use grains that are very different in size, we see more liquid getting stuck in the layers. And if we change how much the grains like water or oil, we find that more liquid of one type gets trapped compared to the other. It is important to understand these small differences to study how fluids move through Earth's layers accurately.

1 Introduction

Carbon dioxide (CO_2) geologic storage has become a pivotal strategy for addressing climate change. During this process, CO_2 is captured from various sources, compressed, and transported before being injected into porous media formations capable of securely retaining the supercritical fluid. Deep saline aquifers represent prime targets for CO_2 storage due to their extensive capacity and global ubiquity (Holloway, 2005; IPCC, 2005; Krevor et al., 2023). Importantly, the sedimentary formations harboring these saline aquifers exhibit inherent natural geological heterogeneities (Bachu, 2003; Eikehaug et al., 2024; Flett et al., 2007; Jackson & Krevor, 2020; Krishnamurthy et al., 2022). Previous studies have shown that centimeter-scale heterogeneities can profoundly influence CO_2 migration and trapping dynamics (Davidson et al., 2022; Krishnamurthy et al., 2017; Trevisan et al., 2015). Therefore, conducting experimental investigations is imperative to quantify the impact of such heterogeneities on trapping performance precisely.

Recent studies, including investigations at pore- and core-scale levels (e.g., micromodels, micro-CT imaging, and core flooding), have been influential in unraveling the intricacies of CO2 fluid behavior within sedimentary rocks (Bakhshian & Hosseini, 2019; Krevor et al., 2011; Krishnamurthy et al., 2017; Kurotori & Pini, 2021; Li & Benson, 2015; Ni et al., 2019; Seyyedi et al., 2022; Trevisan, Gonzalez-Nicolas, et al., 2017; Trevisan, Pini, et al., 2017). However, these studies could only consider the influence of small-scale heterogeneities within their domain sizes, which are limited. In contrast, intermediate tank-scale experiments offer a broader domain size, enabling a more comprehensive characterization of heterogeneity effects. Considerable attention has been devoted to tank-scale experiments to elucidate CO_2 fluid flow dynamics.

For instance, Trevisan et al. (2015) conducted sand tank experiments mimicking an aquifer configuration, demonstrating that dm-scale heterogeneities can increase CO_2 storage capacity through local capillary trapping. In addition, Agartan et al. (2015, 2020) studied the effect of small-scale heterogeneities on dissolution trapping. Their results suggest that dissolved CO_2 remains immobilized below low-permeability zones. Despite the effort to quantify the effect of small-scale heterogeneities through sand tank experiments, such sand configurations do not match realistic sedimentary structures in nature.

Subsequent research entailed multiphase flow tank-scale experiments using an automated feeder machine to replicate realistic heterogeneous conditions. Such tank-scale experimental methods are valuable as they allow engineering of different degrees and types of heterogeneity present in nature. Krishnamurthy et al. (2022) underscored that increased grain size contrast (i.e., degree of heterogeneity) correlates with a higher buoyant flow nonwetting saturation level on cross-bedded formations. Other than cross-beds and herringbone structures (Davidson et al., 2022), no other studies have been conducted on different types of sedimentary domains. However, Ni et al. (2023) demonstrated that heterogeneity geometry can significantly impact the amount of CO_2 capillary trapping. Therefore, in this work, we look at different realistic ripple domains to quantify how variations in bedform patterns affect trapping.

In adjacent research in oil recovery, studies have found that wettability profoundly influences fluid flow dynamics (Masalmeh, 2003; Spiteri et al., 2008). Most sedimentary rocks in deep saline aquifers, notably sandstones, typically exhibit high water-wet characteristics. Nevertheless, these reservoirs may exhibit variability in wettability, which can subsequently impact fluid migration and trapping behaviors (Al-Khdheeawi et al., 2017). Numerous studies have explored pore-scale homogeneous domains to quantify changes in saturation and trapping using techniques such as micro-CT imaging (Celauro et al., 2014; Geistlinger & Ataei-Dadavi, 2015). However, the scientific literature needs more investigations into tank-scale wettability alterations across various types of heterogeneities.

In this study, we assess the impact of modifications in bedform architecture, variations on grain size contrast, and wettability changes in ripple bedforms on trapping performance. Here, we perform capillary- and buoyancy-driven flow experiments within a 3D slab and capture the migration patterns using light transmission techniques. In the following sections, we discuss the fluid flow dynamics regarding ripple domains and the effect of the degree of heterogeneity and wettability on trapped saturation. Additionally, we explored the implications of such variations on capillary heterogeneity trapping.

2 Experimental Overview

Realistic heterogeneities found in nature are selected from Rubin and Carter (2006) bedform architecture models. For this study, we choose ripple patterns consisting of two different facies: matrix (coarse grains) and laminae (fine grains). The patterns are packed using glass beads of different diameters with an automated feeding system in a 3D slab chamber (60 x 60 x 2 cm^3) (Krishnamurthy et al., 2019). The height of the heterogeneous portion of the domain is approximately 42 cm.

Glass beads with varying degrees of wettability are used. The wettability of the glass beads was estimated by measuring the contact angle between the beads and water (Guo et al., 2023; Hernandez, 2011; Wang & Tokunaga, 2015).

The multiphase flow experiments consist of drainage and redistribution, with both stages at atmospheric conditions with inlet constant rate and outlet constant pressure. Heptane (i.e., nonwetting phase) (S_{nw}) and a glycerol-water mixture (i.e., wetting phase) are used as analog fluids for supercritical CO_2 and in-situ brine, respectively (Krishnamurthy et al., 2019; Ni & Meckel, 2021). To prepare for the experiment, the chamber is filled with the glycerol-water mixture at high flow rates to dissolve gaseous CO_2, previously injected to displace air inside the tank, until the mixture flows out from the outlet reservoir.

During the drainage phase, heptane is injected from the bottom middle inlet of the chamber at a low flow rate (0.2 ml/min) to guarantee that the flow is gravity- and capillary-driven. The injection continues for 24 hours after heptane leaves the chamber. Redis-

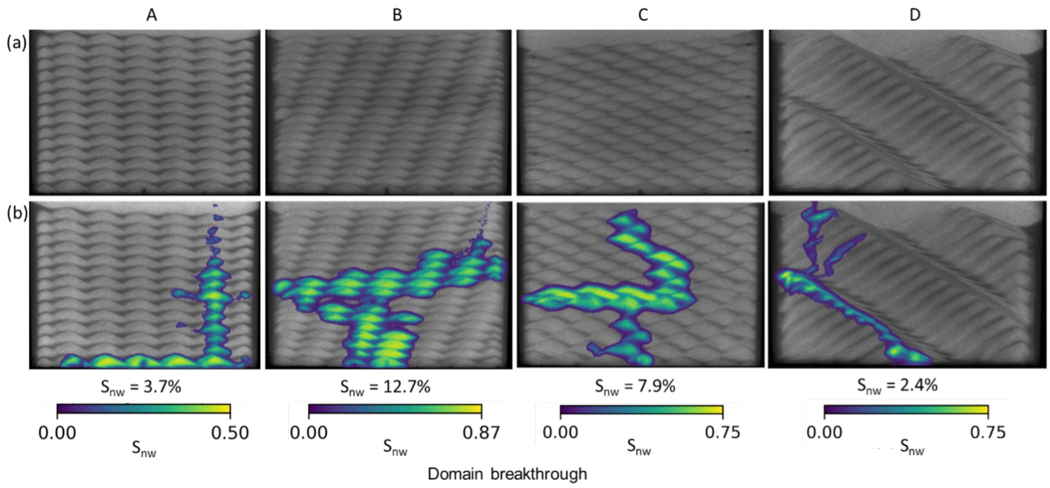

Figure 1. Figure 1. (a) Ripple domain patterns with slight changes in the ripple crest phase. A: in-phase, B: slightly out-of-phase, C: out-of-phase, and D: large out-of-phase. (b) Breakthrough nonwetting phase saturation field and domain average saturation values for all patterns. The color bar shows pixel-wise nonwetting saturation.

tribution happens immediately after stopping the injection and lasts for 24 hours. A light transmission visualization technique (Bob et al., 2008; Darnault et al., 1998; DiCarlo, 2004; Krishnamurthy et al., 2022; Niemet et al., 2002; Tidwell & Glass, 1994; Weisbrod et al., 2003) is used throughout the entire experiment to capture the nonwetting phase saturation. Saturation fields are recorded every 30 seconds for the drainage stage and every 30 minutes for the redistribution stage. We report three saturation fields taken throughout the experiment: at heterogeneous domain breakthrough, the end of injection (drainage), and the end of redistribution.

We conduct three sets of experiments in the study. Firstly, different ripple bedform architectures are packed (in-phase, slightly out-of-phase (i.e., climbing), out-of-phase, and large climbing ripples) with constant grain size contrast between the matrix and the laminae facies. Secondly, in-phase ripples with varying grain size contrast are filled to validate previously obtained results on a cross-laminated bedform architecture (Krishnamurthy et al., 2022). Thirdly, ripple bedforms architecture with constant grain size contrast and different wettability (water- to oil-wet).

3 Results

3.1 Changes in bedform architecture

Figure 1a shows the four ripple patterns (A to D) that we used – there are slight modifications on the ripple crest phases between layers, and Experiment D also shows an increase in ripple size. Figure 1b shows the 2D nonwetting phase saturation for each bedform at breakthrough. We observe that a slight displacement in ripple phases allowed the nonwetting phase to extend farther laterally and accumulate in more layers. The combined effect increases the nonwetting phase saturation in the heterogeneous domain and changes the migration pattern from fingering to more capillary heterogeneity trapping behind capillary barriers.

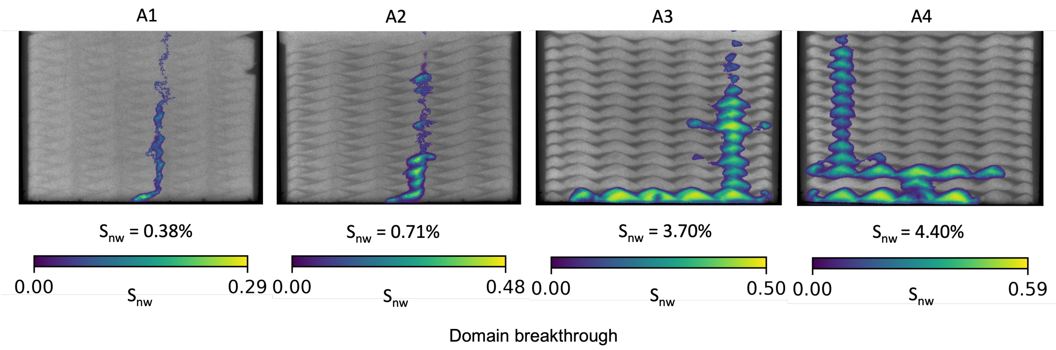

Figure 2. Figure 2. Nonwetting phase saturation field and domain average saturation values at breakthrough for in-phase ripples with increasing degree of heterogeneity (A1 to A4). The color bar shows pixel-wise nonwetting saturation.

3.2 Changes in grain size contrast

In addition to the multiple ripple bedform architectures, experiments with varying grain size contrast for the in-phase ripple pattern were performed. Figure 2 shows the breakthrough nonwetting saturation field with grain size contrast increasing from A1 to A4. When the size contrast between the coarse and fine grains is small (A1 and A2), the nonwetting phase fluid breaks through the domain as a finger quickly. At higher contrast (A3 and A4), the fluid builds up column height beneath the laminae and extends laterally until a zone of low capillary entry pressure is reached to move up into the upper layers. Increasing grain size contrast leads to more nonwetting phase saturation trapped within the heterogeneous domain.

3.3 Changes in wettability

Besides conducting experiments on the type and degree of heterogeneity, we ran experiments in ripple patterns to study the effect of wettability on nonwetting phase saturation. Glass beads with variations in contact angle were selected. Note that only the wettability of the matrix (coarse) changed, while the laminae (fine) remained water-wet for all experiments. The domain and grain size contrast were also kept constant. Water- and intermediate-wet experiments were filled entirely by the wetting phase. However, during water injection, the oil-wet scenarios had gas bubbles trapped within the domain because of the affinity of the beads to retain gas during experiment preparation. Figure 3 shows the nonwetting phase saturation at breakthrough for in-phase and out-of-phase ripples with different contact angles.

3.4 Total trapped saturation

Although we measure the saturation field throughout each experiment, here, we summarize the total trapped saturation at the end of drainage. This is slightly higher than the breakthrough saturation as new migration pathways are formed during the drainage stage, which leads to more fluid accumulation pools. Figure 4 shows drainage saturations as a function of the type of heterogeneity, degree of heterogeneity, and contact angle. The dimensionless parameter δ is used to capture the degree of heterogeneity of the bedforms and is a function of the mean and standard deviation of the matrix and laminae (Krishnamurthy et al., 2022).

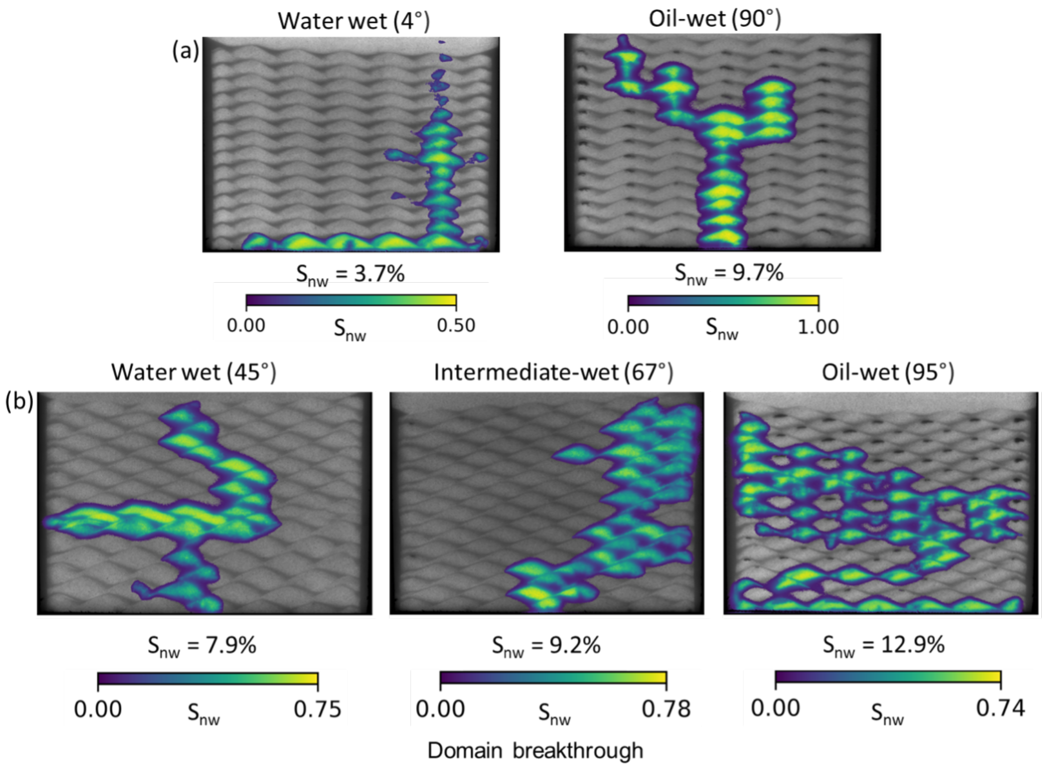

Figure 3. Figure 3. Heptane (representing supercritical CO_2) saturation field and domain average saturation values at breakthrough for in-phase (a) and out-of-phase (b) ripples with varying wettability. The color bar shows pixel-wise nonwetting saturation.

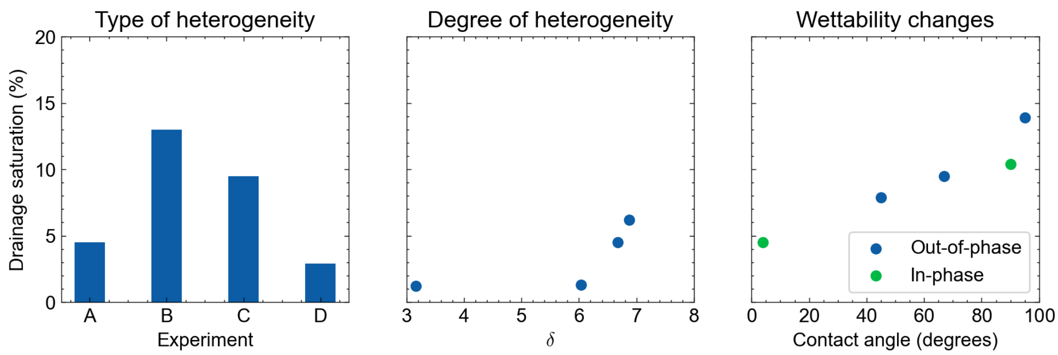

Figure 4. Figure 4. Domain average drainage saturation versus type of heterogeneity, degree of heterogeneity, and contact angle.

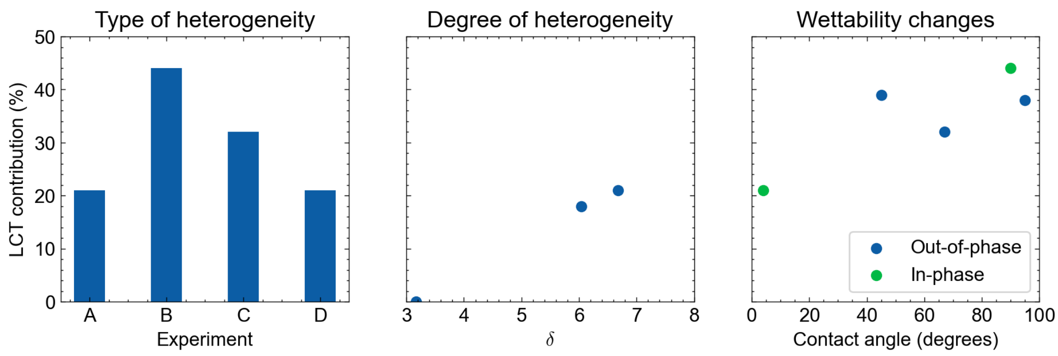

Figure 5. Figure 5. Contribution of CHT to total trapping as a function of the type of heterogeneity, degree of heterogeneity, and contact angle.

3.5 Capillary heterogeneity trapping

After the redistribution stage, some regions below capillary barriers exhibit a saturation greater than residual. This excess saturation is known as local capillary trapping or capillary heterogeneity trapping (CHT). Residual saturation for homogeneous water-wet glass beads can be assumed to be within the range of 0.16–0.25 (Chatzis et al., 1983; Dullien et al., 1989; Mayer & Miller, 1992). The CHT contribution was computed as the average pixel-level ratio of the difference between redistribution and residual saturation (assumed 0.25) over redistribution saturation (Krishnamurthy et al., 2022). Figure 5 shows the percentage contribution of CHT to total trapping as a function of the type of heterogeneity, degree of heterogeneity, and contact angle.

4 Discussion

In this and the following subsections, we analyze the results further and discuss potential reasons for and implications of our observations.

4.1 Fluid flow dynamics in ripple bedforms

We observe that the phase of the ripples (patterns A through C) changes the amount of trapped saturation after drainage and redistribution. To understand why, we first describe the dynamics of the ripples that were created. When ripples are built by the automated feeder apparatus, beads will tend to roll down from the crest to the trough because of gravity. Therefore, a thinner laminae barrier is produced at the crest, potentially leaving gaps in the fine media and a lower capillary entry pressure. The latter can be observed in Figure 1a, where the sides of the ripples show a darker color compared to the crest. This dark color is a consequence of fine bead accumulation.

In the case of in-phase ripples (A), all the ripple crests will be aligned on top of each other. The fluid moves laterally during injection until it builds sufficient column height to percolate to the upper layer. Generally, for in-phase ripples, the fluid will migrate following a preferential flow pathway through the similar crest location in all layers, thus leading to a low breakthrough and drainage nonwetting saturation.

On the other hand, out-of-phase ripples can be slightly or entirely unaligned, meaning that crests will tend to be aligned with troughs, creating potentially high capillary entry pressure barriers that increase breakthrough and drainage nonwetting saturation. Nonetheless, there is no trend for how crest phase-shifting influences saturation as slightly out-of-phase ripples (B) present higher nonwetting saturation than completely out-of-

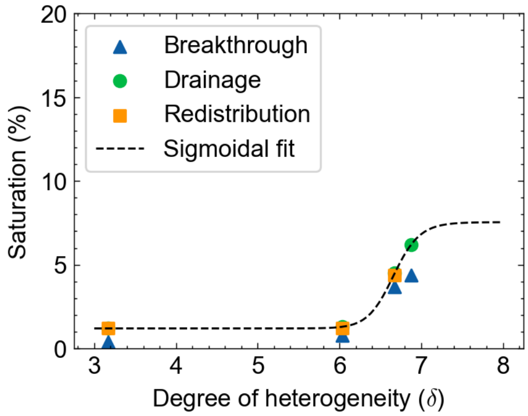

Figure 6. Figure 6. Overall nonwetting phase saturation after each experiment stage as a function of the degree of heterogeneity. The dashed line represents the S-shaped curve fitted to the drainage saturation, as Krishnamurthy et al. (2022) demonstrated.

phase (C). In the case of large climbing ripples (D), the sides of the crests are aligned in each layer, building a thicker diagonal lamination with high capillary entry pressure. Once the fluid reaches the lamination, it preferentially flows underneath such barriers until it migrates to the adjacent ripple layer.

As a result, various ripple patterns will exhibit different breakthrough and drainage nonwetting saturation (Figure 4). Such flow dynamics behavior will also have implications on CHT. Slight changes in ripple bedform can increment 10 to 20% the contribution of CHT, as shown in Figure 5.

4.2 The effect of the grain size contrast in ripple bedforms

Previously, Krishnamurthy et al. (2022) demonstrated that an increase in grain size contrast leads to a higher nonwetting phase saturation when measured in cross-bedded heterogeneities. Saturation increases until it reaches a plateau at a higher degree of heterogeneity. This behavior in saturation can be modeled as a sigmoidal S-shaped curve as a function of the dimensionless parameter δ (function of the mean and standard deviation of the matrix and laminae). We apply the same analysis to in-phase ripple domains measured here, and we find similar behavior. Figure 6 displays the domain average nonwetting saturation at each experiment stage as a function of the degree of heterogeneity. For this bedform architecture, nonwetting phase saturation increases until it reaches a plateau of approximately 8%. Further, an increase in the degree of heterogeneity will increase CHT contribution until a plateau of 20% is reached at higher degree contrasts (Figure 5).

Both saturation and CHT plateaus differ from cross-bedded formation values (34% and 80%, respectively). These results suggest that the structural complexity of the heterogeneity controls the plateau, as saturation and CHT differ from one bedform architecture to another.

4.3 The effect of wettability changes in ripple bedforms

In addition to the type and degree of heterogeneity, wettability alterations can also impact the trapped saturation within the heterogeneous domain. These alterations in wettability promote lateral migration and discourage vertical displacement in ripple bedforms, as shown in Figure 3. Thus, it increases the domain sweep efficiency, hence, the overall saturation.

Ripple bedforms show a monotonic relation between contact angle and saturation (Figure 4). As a result, an increase of approximately 5% in drainage saturation when shifting from water- to oil-wet beads is observed. Nevertheless, during water injection, oil-wet scenarios (Figure 3) have gas bubbles trapped inside the domain because of the tendency of the beads to retain gas. The presence of the bubbles will reduce nonwetting saturation because (a) gas will reduce the pore space available to the nonwetting phase as it migrates, and (b) gas will decrease the necessary nonwetting phase column height to overcome the capillary entry pressure of the beads because the gas column itself has a higher buoyancy force. The latter suggests that more nonwetting phase saturation can be achieved in oil-wet ripples.

Such monotonic behavior is also exhibited in the contribution of CHT to total trapping (Figure 5). However, this trend can be significantly modified by the type of heterogeneity variations. In the case of in-phase ripples, as the water-wet domain shifts to oil-wet, the contribution of CHT increases by approximately 20%. On the other hand, CHT contribution on out-of-phase ripples, independent of contact angle, remains close to 40%.

4.4 Trapping efficiency: Initial-Residual scatter plots

During the redistribution stage under hydrostatic conditions, we observe that the nonwetting phase escapes the domain, decreasing saturation. However, most of the fluid remains trapped inside the domain. Thus, the trapped nonwetting phase is highly correlated with the drainage saturation. To evaluate the trapping performance, we plot Initial – Residual (IR) plots, which are commonly used to generate parametric trapping models (Krevor et al., 2015; Krishnamurthy et al., 2022; Ni et al., 2019; Spiteri et al., 2008). Our slab-scale experiment allows us to plot this on a pixel-by-pixel basis. Figure 7 shows the pixel-level redistribution saturation as a function of the drainage saturation for the type of heterogeneity (a), degree of heterogeneity (b), and wettability changes (c). Moreover, the ratio between redistribution and drainage average saturation was estimated to quantify the domain trapping efficiency percentage (shown in parenthesis). Finally, the Land trapping model was fitted to all experimental results. Land coefficient (C) equal to zero (i.e., 100% efficiency) represents that the nonwetting phase remains trapped after redistribution. Therefore, higher values of C indicate worse trapping performance. Experiment A4 lacks redistribution saturation and thus is excluded from this analysis.

4.5 Impact of type and degree of heterogeneity, and wettability changes on trapping performance

The scatter shape of the IR plots differs between ripple patterns, as shown in Figure 7a. This observation suggests an interplay between domain heterogeneity type and trapping performance. In the ripple pattern case, a slight shift in the crest leads to a decrease in trapping efficiency. When the amount of scatter increases above the 100% trapping line (C=0), a high trapping efficiency is expected, as the fluid redistributes within the domain and remains trapped. Conversely, a low trapping efficiency is expected for domains with increasing scatter below the 100% trapping line, where the nonwetting phase redistributes and escapes the domain.

Figure 7b shows that an increase in the degree of heterogeneity provokes a higher amount of scatter, which leads to variation in trapping performance. Changes in the degree of heterogeneity do not show a concrete trend in trapping efficiency. Since the amount of scatter is balanced on both sides of the 100% trapping line, this explains why in-phase ripples, independent of grain size contrast, will exhibit trapping efficiencies above 90%.

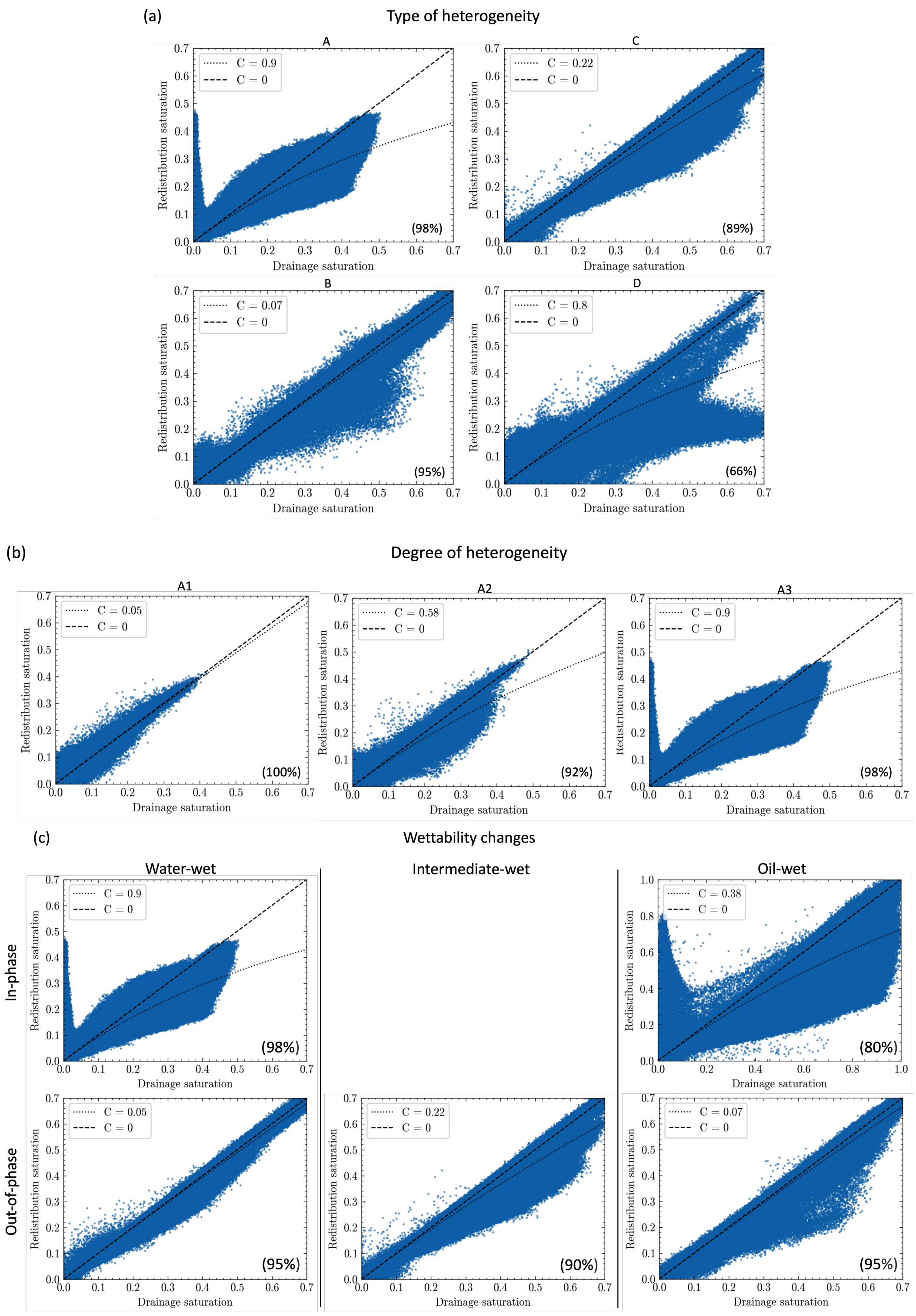

Figure 7. Figure 7. Pixel-wise redistribution nonwetting saturation as a function of drainage saturation for the type of heterogeneity (a), degree of heterogeneity (b), and wettability (c). The dashed line shows 100% trapping (C=0), and the dotted line depicts the domain average Land trapping coefficient. Values in parenthesis represent the trapping efficiency as the overall redistribution and drainage saturation ratio.

An increase in fitted C is expected as a high degree of heterogeneity allows for more fluid redistribution (Krishnamurthy et al., 2022).

However, more care should be taken when using the Land trapping model to define trapping performance. A higher domain C value can indicate nonwetting phase redistributing within the domain (i.e., higher CHT contribution). Thus, a considerable CHT contribution can significantly impact the Land trapping model as the model is designed to fit pore-scale residual trapping data better.

Finally, we observed in Figure 7c that the scatter shape of the IR plots remains constant when the type and degree of heterogeneity are unaltered. However, the amount of scatter increment in the IR plots is because of the domain matrix wettability variation from water to oil-wet. The previous observations demonstrate that the trapping performance of the domain is highly correlated with the domain wettability. Fitted domain C values do not consider the heterogeneous wettability throughout the domain (assumed homogeneous), which can lead to an inaccurate Land trapping coefficient.

5 Summary and Conclusions

In this study, we conduct tank-scale multiphase flow experiments in various ripple pattern domains with variations in grain size contrast and domain matrix wettability to quantify their effects on saturation, capillary heterogeneity trapping, and overall trapping performance. We demonstrate that slight changes in bedform architecture can significantly impact nonwetting saturation. Moreover, we found that capillary heterogeneity trapping is highly dependent on the type of heterogeneity, as subtle changes in ripple patterns can increment CHT by $10 - 20\%$. Additionally, we have corroborated that an increase in grain size contrast between matrix and laminae increases nonwetting saturation, as Krishnamurthy et al. (2022) proposed for cross-bedded formations. We validated that an increase in the contribution of CHT is expected at higher degree contrasts. Finally, our findings on wettability changes on the domain matrix facies suggest that with a shift from water- to oil-wet grains, a 5% increase in nonwetting saturation can be achieved, and an increment of 10% to 20% on CHT contribution can be expected.

Open Research Section

The experimental data in the study are available at UT-Austin Dataverse via `https://dataverse.tdl.org/dataverse/ripplebedform`

Disclaimer

This report was prepared as an account of work sponsored by an agency of the United States Government. Neither the United States Government nor any agency thereof, nor any of their employees, makes any warranty, express or implied, or assumes any legal liability or responsibility for the accuracy, completeness, or usefulness of any information, apparatus, product, or process disclosed, or represents that its use would not infringe privately owned rights. Reference herein to any specific commercial product, process, or service by trade name, trademark, manufacturer, or otherwise does not necessarily constitute or imply its endorsement, recommendation, or favoring by the United States Government or any agency thereof. The views and opinions of authors expressed herein do not necessarily state or reflect those of the United States Government or any agency thereof.

Acknowledgments
This work was supported by the Energy Institute at The University of Texas at Austin through the Energy Seed Grant and by the U.S. Department of Energy through the Gulf of Mexico Partnership for Offshore Carbon Storage under grant award number DE-FE0031558.

Special thanks to Mason Fleming for his splendid work during his Summer Research Internship Experience (SURI) funded by the Hildebrand Department of Petroleum and Geosystems Engineering at The University of Texas at Austin.

References

Agartan, E., Illangasekare, T. H., Vargas-Johnson, J., Cihan, A., & Birkholzer, J. (2020). Experimental investigation of assessment of the contribution of heterogeneous semi-confining shale layers on mixing and trapping of dissolved co_2 in deep geologic formations. *International Journal of Greenhouse Gas Control*, *93*. doi: https://doi.org/10.1016/j.ijggc.2019.102888

Agartan, E., Trevisan, L., Cihan, A., Birkholzer, J., Zhou, Q., & Illangasekare, T. H. (2015). Experimental study on effects of geologic heterogeneity in enhancing dissolution trapping of supercritical co_2. *Water Resources Research*, 1635-1648. doi: https://doi.org/10.1002/2014WR015778

Al-Khdheeawi, E. A., Vialle, S., Barifcani, A., Sarmadivaleh, M., & Iglauer, S. (2017). Impact of reservoir wettability and heterogeneity on co_2 plume migration and trapping capacity. *International Journal of Greenhouse Gas Control*, *58*, 142-158. doi: http://dx.doi.org/10.1016/j.ijggc.2017.01.012

Bachu, S. (2003, 6). Screening and ranking of sedimentary basins for sequestration of co_2 in geological media in response to climate change. *Environmental Geology*, *44*, 277-289. doi: 10.1007/s00254-003-0762-9

Bakhshian, S., & Hosseini, S. A. (2019, 4). Pore–scale analysis of supercritical co_2-brine immiscible displacement under fractional–wettability conditions. *Advances in Water Resources*, *126*, 96-107. doi: 10.1016/J.ADVWATRES.2019.02.008

Bob, M. M., Brooks, M. C., Mravik, S. C., & Wood, A. L. (2008, 5). A modified light transmission visualization method for dnapl saturation measurements in 2-d models. *Advances in Water Resources*, *31*, 727-742. doi: 10.1016/j.advwatres.2008.01.016

Celauro, J. G., Torrealba, V. A., Karpyn, Z. T., Klise, K. A., & Mckenna, S. A. (2014, 2). Pore-scale multiphase flow experiments in bead packs of variable wettability. *Geofluids*, *14*, 95-105. doi: 10.1111/gfl.12045

Chatzis, J., Morrow, N., & Lim, H. (1983). Magnitude and detailed structure of residual oil saturation. *SPE Journal*, *23*, 311-326. doi: https://doi.org/10.2118/10681-PA

Darnault, C. J., Throop, J. A., Dicarlo, D. A., Rimmer, A., Steenhuis, T. S., & Parlange, J. Y. (1998, 6). Visualization by light transmission of oil and water contents in transient two-phase flow fields. *Journal of Contaminant Hydrology*, *31*, 337-348. doi: 10.1016/S0169-7722(97)00068-5

Davidson, M. A., Mumford, K. G., Mullins, N., & Calvert, M. M. (2022). Modification of a 3d printer to create geologically realistic heterogeneous sand packs. *Vadose Zone Journal*. doi: 10.1002/vzj2.20216

DiCarlo, D. A. (2004). Experimental measurements of saturation overshoot on infiltration. *Water Resources Research*, *40*. doi: 10.1029/2003WR002670

Dullien, F. A. L., Zarcone, C., Macdonald, I. F., Collins, A., & Bochard, R. D. E. (1989). The effects of surface roughness on the capillary pressure curves and the heights of capillary rise in glass bead packs. *Journal of Colloid and Interface Science*, *127*, 362-372. doi: https://doi.org/10.1016/0021-9797(89)90042-8

Eikehaug, K., Haugen, M., Folkvord, O., Benali, B., Larsen, E. B., Tinkova, A., . . . Fernø, M. A. (2024). Engineering meter-scale porous media flow experiments for quantitative studies of geological carbon sequestration. *Transport in Porous Media*. doi: 10.1007/s11242-023-02025-0

Flett, M., Gurton, R., & Weir, G. (2007, 5). Heterogeneous saline formations for carbon dioxide disposal: Impact of varying heterogeneity on containment and trapping. *Journal of Petroleum Science and Engineering*, *57*, 106-118. doi: 10.1016/j.petrol.2006.08.016

Geistlinger, H., & Ataei-Dadavi, I. (2015). Influence of the heterogeneous wettability on capillary trapping in glass-beads monolayers: Comparison between experiments and the invasion percolation theory. *Journal of Colloid and Interface Science*, *459*, 230-240. Retrieved from `http://dx.doi.org/10.1016/j.jcis.2015.07.074` doi: 10.1016/j.jcis.2015.07.074

Guo, Y., Shi, Y., & Mohanty, K. (2023). Improvement of polymer flooding of a viscous oil by addition of an alkali.. doi: https://doi.org/10.2118/215108-MS

Hernandez, A. (2011). *Observations of buoyant plumes in countercurrent displacement* . The University of Texas at Austin.

Holloway, S. (2005). Underground sequestration of carbon dioxide-a viable greenhouse gas mitigation option. *Energy*, *30*, 2318-2333. doi: 10.1016/j.energy.2003.10.023

IPCC. (2005). *Special report on carbon dioxide capture and storage* (Tech. Rep.).

Jackson, S. J., & Krevor, S. (2020, 9). Small-scale capillary heterogeneity linked to rapid plume migration during co2 storage. *Geophysical Research Letters*, *47*. doi: 10.1029/2020GL088616

Krevor, S., Blunt, M. J., Benson, S. M., Pentland, C. H., Reynolds, C., Al-Menhali, A., & Niu, B. (2015, 1). Capillary trapping for geologic carbon dioxide storage - from pore scale physics to field scale implications. *International Journal of Greenhouse Gas Control*, *40*, 221-237. doi: 10.1016/j.ijggc.2015.04.006

Krevor, S., Coninck, H. D., Gasda, S. E., Ghaleigh, N. S., Gooyert, V. D., Hajibeygi, H., . . . Swennenhuis, F. (2023). Subsurface carbon dioxide and hydrogen storage for a sustainable energy future. *Nature Reviews Earth Environment —*, *4*, 102-118. doi: 10.1038/s43017-022-00376-8

Krevor, S., Pini, R., Li, B., & Benson, S. M. (2011). Capillary heterogeneity trapping of co_2 in a sandstone rock at reservoir conditions. *Geophysical Research Letters*, *38*. doi: 10.1029/2011GL048239

Krishnamurthy, P. G., DiCarlo, D., & Meckel, T. (2022). Geologic heterogeneity controls on trapping and migration of co_2. *Geophysical Research Letters*, *49*. doi: 10.1029/2022GL099104

Krishnamurthy, P. G., Meckel, T. A., & DiCarlo, D. (2019). Mimicking geologic depositional fabrics for multiphase flow experiments. *Water Resources Research*, *55*, 9623-9638. doi: 10.1029/2019WR025664

Krishnamurthy, P. G., Senthilnathan, S., Yoon, H., Thomassen, D., Meckel, T., & DiCarlo, D. (2017). Comparison of darcy's law and invasion percolation simulations with buoyancy-driven co2-brine multiphase flow in a heterogeneous sandstone core. *Journal of Petroleum Science and Engineering*, *155*, 54-62. doi: 10.1016/J.PETROL.2016.10.022

Kurotori, T., & Pini, R. (2021). A general capillary equilibrium model to describe drainage experiments in heterogeneous laboratory rock cores. *Advances in Water Resources*, *152*. doi: 10.1016/j.advwatres.2021.103938

Li, B., & Benson, S. M. (2015). Influence of small-scale heterogeneity on upward co_2 plume migration in storage aquifers. *Advances in Water Resources*, *83*, 389-404. doi: 10.1016/j.advwatres.2015.07.010

Masalmeh, S. K. (2003). The effect of wettability heterogeneity on capillary pressure and relative permeability. *Journal of Petroleum Science and Engineering*, *39*, 399-408. doi: 10.1016/S0920-4105(03)00078-0

Mayer, A., & Miller, C. (1992). The influence of porous medium characteristics and measurement scale on pore-scale distributions of residual nonaqueous-phase liquids. *Journal of Contaminant Hydrology*, *11*, 189-213.

Ni, H., Bakhshian, S., & Meckel, T. A. (2023). Effects of grain size and small-scale bedform architecture on co_2 saturation from buoyancy-driven flow. *Scientific*

Reports, *13*. doi: 10.1038/s41598-023-29360-y

Ni, H., Boon, M., Garing, C., & Benson, S. M. (2019). Predicting co_2 residual trapping ability based on experimental petrophysical properties for different sandstone types. *International Journal of Greenhouse Gas Control*, *86*, 158-176. doi: 10.1016/j.ijggc.2019.04.024

Ni, H., & Meckel, T. A. (2021). Characterizing the effect of capillary heterogeneity on multiphase flow pulsation in an intermediate-scale beadpack experiment using time series clustering and frequency analysis. *Water Resources Research*, *57*. doi: 10.1029/2021WR030876

Niemet, M. R., Rockhold, M. L., Weisbrod, N., & Selker, J. S. (2002, 8). Relationships between gas-liquid interfacial surface area, liquid saturation, and light transmission in variably saturated porous media. *Water Resources Research*, *38*, 10-1-10-12. doi: 10.1029/2001wr000785

Rubin, D. M., & Carter, C. L. (2006). *Cross-bedding, bedforms, and paleocurrents* (Second ed., Vol. 1).

Seyyedi, M., Clennell, M. B., & Jackson, S. J. (2022). Time-lapse imaging of flow instability and rock heterogeneity impacts on co_2 plume migration in meter long sandstone cores. *Advances in Water Resources*, *164*. doi: 10.1016/j.advwatres.2022.104216

Spiteri, E. J., Juanes, R., Blunt, M. J., & Orr, F. (2008). A new model of trapping and relative permeability hysteresis for all wettability characteristics. *SPE Journal*, *3*, 277-288.

Tidwell, V. C., & Glass, R. J. (1994). X ray and visible light transmission for laboratory measurement of two-dimensional saturation fields in thin-slab systems. *Water Resources Research*, *30*, 2873-2882. doi: 10.1029/94WR00953

Trevisan, L., Gonzalez-Nicolas, A., Cihan, A., Pini, R., Birkholzer, J., & Illangasekare, T. (2017). Experimental and modeling study of capillary/buoyancy-driven flow of surrogate co2 through intermediate-scale sand tanks. *Energy Procedia*, *114*, 5032-5037. doi: 10.1016/J.EGYPRO.2017.03.1653

Trevisan, L., Pini, R., Cihan, A., Birkholzer, J. T., Zhou, Q., Gonzalez-Nicolas, A., & Illangasekare, T. H. (2017). Imaging and quantification of spreading and trapping of carbon dioxide in saline aquifers using meter-scale laboratory experiments. *Water Resources Research*, 485-582. doi: 10.1002/2016WR019749

Trevisan, L., Pini, R., Cihan, A., Birkholzer, J. T., Zhou, Q., & Illangasekare, T. H. (2015, 11). Experimental analysis of spatial correlation effects on capillary trapping of supercritical co2 at the intermediate laboratory scale in heterogeneous porous media. *Water Resources Research*, *51*, 8791-8805. doi: 10.1002/2015WR017440

Wang, S., & Tokunaga, T. K. (2015, 6). Capillary pressure-saturation relations for supercritical co2 and brine in limestone/dolomite sands: Implications for geologic carbon sequestration in carbonate reservoirs. *Environmental Science and Technology*, *49*, 7208-7217. doi: 10.1021/acs.est.5b00826

Weisbrod, N., Niemet, M. R., & Selker, J. S. (2003, 8). Light transmission technique for the evaluation of colloidal transport and dynamics in porous media. *Environmental Science and Technology*, *37*, 3694-3700. doi: 10.1021/es034010m